

## Effects of Fire Cycle Time on Heat Transfer Characteristics and Energy Consumption in Anode Baking Furnace

Abdul Raouf Tajik<sup>1</sup>, Rashid K. Abu Al-Rub<sup>2</sup>, Mouna Zaidani<sup>3</sup>, Zahid Ahmed Qureshi<sup>4</sup>  
and Tariq Shamim<sup>5</sup>

1. Ph.D. Student

2. Department Head and Associate Professor

3. Postdoctoral Researcher

4. MSc. Student

5. Professor

Institute Center for Energy (iEnergy), Department of Mechanical and Materials Engineering,  
Khalifa University of Science and Technology, Masdar Institute, Abu Dhabi, U.A.E.

Corresponding author: tshamim@masdar.ac.ae

### Abstract

Anode Baking is an expensive and a very important step during carbon anode production. Numerical modeling is an imperative tool to investigate the effect of different parameters on anode baking process. In the present study, a high-fidelity and novel computational software ABKA (Anode Baking Kiln Analysis) has been developed which simulates heat transfer and flow distributions of the entire anode baking process. Fire cycle (*FC*) determines the production output of a kiln. Faster *FC* produces more anodes while slower *FC* slows down anode production. But both extremes have limitations. Using ABKA, effects of varying *FC* with different average flue-gas soaking temperature and flue-gas soaking time are studied. The results are expressed in terms of fuel consumption, and anode maximum, minimum and average temperature for each layer of anode-pack separately. Furthermore, the baking uniformity for each case is quantified. Considering multiple factors, desirable combinations of *FC*, soaking time, and soaking temperature can be identified. Finally, for varying *FC*, soaking time, and soaking temperature, it is observed that by increasing *FC*, baking homogeneity can be improved with a slight increase in fuel consumption; however, higher *FC* reduces the furnace production which should be taken into consideration at the same time.

**Keywords:** Anode-baking, fire cycle time, soaking temperature, soaking time, packing coke.

### 1. Introduction

In aluminium industry, for each ton of aluminium to be produced approximately 0.4 ton of carbon anodes are consumed in the reduction cell. Green (unbaked) anodes should be baked (heat treated) in advance to obtain particular mechanical, thermal and electrical properties that make them suitable to be used as anode in the aluminium production process. The anode baking process takes generally 390-480 hours, and several phenomena occur during the process. Effects of operational-geometrical parameters on the performance of the furnace by plant tests are usually expensive and disrupt the baking process. Therefore, numerical-mathematical modelling is an imperative tool to study the effect of different parameters on the anode quality and furnace performance. Ultimately the optimum baking process and furnace geometry can be proposed. Several studies on modelling the anode baking process are reported in the literature [1-14]. The main objectives of the developed computational model are to study the effect of material properties on the baking process, to investigate the effect of various parameters on anode temperature distribution, and to investigate the temperature evolution through the width of the pit.

## 2. Model Description

Anode baking furnace is a circular kiln with pits, analogous to a closed chain. As shown in Figure 1, a fire group usually consists of three preheating sections, three firing sections, six cooling sections, one unloading section, one or two sections for the loading of green anodes and one or two sections for the sake for maintenance. After each fire cycle time (typically 24-32 hours), the fire group equipment is displaced one section forward in the direction of the fire advance which is typically clockwise direction. A furnace comprises of two fire groups where the sections are arranged in two rows side by side, joined at the two ends by the crossover. The fire advance direction and the flow direction of combustion air and flue gases in the flue walls is the same. Simulating this intermittent movement of the fire group along with all the other simultaneous and transient phenomena involved in the baking process is very challenging and at the same time computationally very intensive since the initial and boundary conditions are continuously varying from one section to another. In a view to overcome this difficulty, all the sections from preheating, firing to cooling are treated as a whole and the baking furnace is assumed to be a semi-continuous counter flow heat exchanger between the stepwise movement of the solids in the pit and continuous flow of the gas in the flue. However, to avoid the virtual movement of the anodes, the solids are fictitiously subdivided into a number of finite slices along the length of the furnace. The velocity of the gas is varying and is determined by considering the local mass flow rate, temperature and pressure. The constant velocity of the solids is equal to a section length divided by the fire cycle time (about 5 m per day).

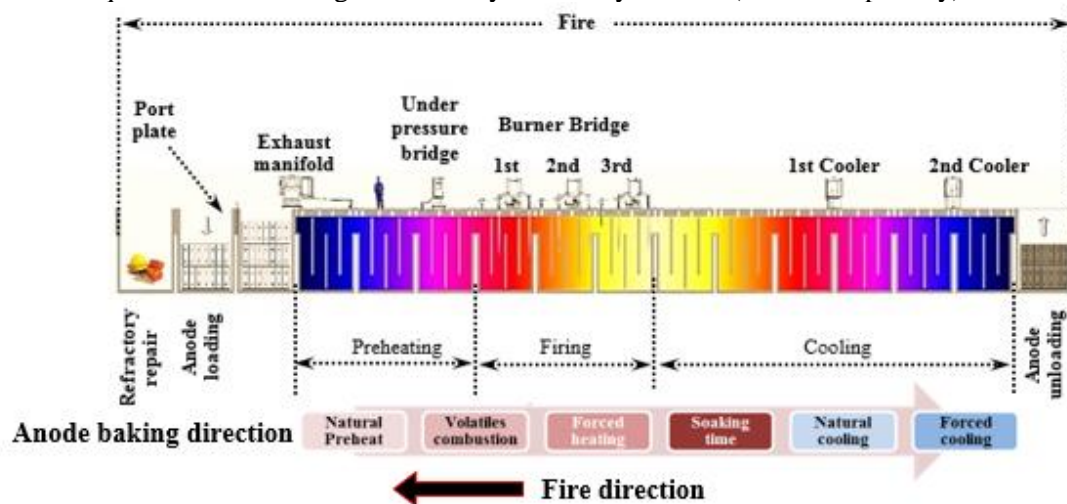


Figure 1. Longitudinal view of all the sections in a fire group [9].

### 2.1. Coupling of the flue and pit models

The transient nature of the anode baking process should be taken into consideration while developing the computational algorithms for the model. Assuming symmetry, only half of the flue and half of the pit can be considered for the computation. The time scale of the gas is much smaller than that of the solid materials (i.e. the solid components take more time to respond to changes in boundary conditions whereas gas responds to variations quickly). Combustion of fuel and volatiles in the flue along with gas flow combined with air in-leakage and ex-leakage can be modelled independent of time. However, the transient (time-dependent) heat conduction equation should be solved for the pit sub-model (i.e., heat transfer through the flue-wall, packing coke, and anode pack). Thus, the developed numerical model consists of two sub-models: flue and pit (flue-wall, packing coke, and anode pack). As shown in Figure 2, the pit

model and flue model are developed separately and then coupled through an interface located at the refractory wall surface on the flue side.

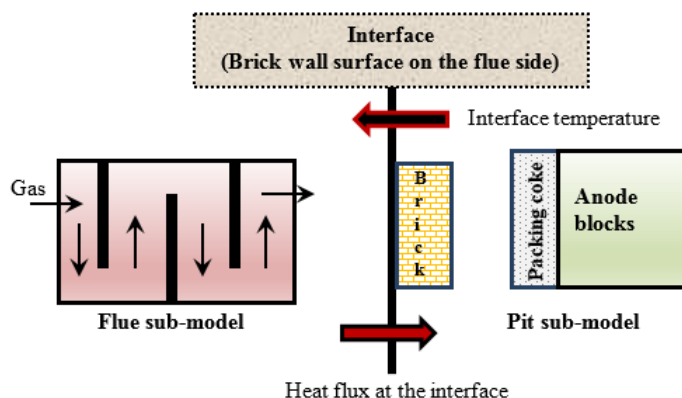


Figure 2. Coupling of the flue and pit sub-models.

## 2.2. Governing equations

The followings are the governing equations that are solved for the modelling of the anode baking process. Figure 4-a, shows schematic view of 1D domain for heat conduction in the traversal direction, perpendicular to fire direction. 1D transient heat conduction equation can be written as:

$$\rho_s C_{ps} \frac{\partial T_s}{\partial t} = \frac{\partial}{\partial y} \left( k_s \frac{\partial T_s}{\partial y} \right) + \frac{\partial}{\partial z} \left( k_s \frac{\partial T_s}{\partial z} \right) \quad (1)$$

Where,

- $k_s$  Thermal conductivity of the solids (wall, packing coke and anodes), W/m. °C
- $C_{ps}$  Specific heat of the solids, J/kg. °C
- $\rho_s$  Density of the solids, kg/m<sup>3</sup>
- $T_s$  Solids temperature, °C
- $t$  Time, (s)
- $y$  Transversal co-ordinate perpendicular to the fire direction, m

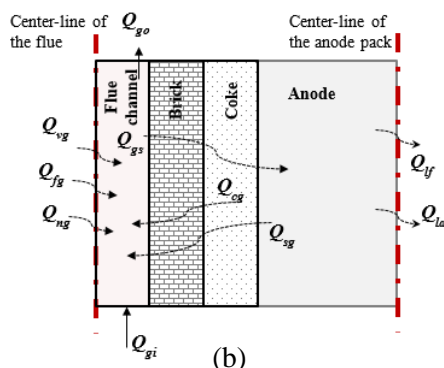


Figure 3. Schematic of the gas control volume.

The adiabatic boundary condition is adopted for the axis of the symmetry at the centre of the anode. The interface between flue-gas and refractory wall is treated as convective-radiative

boundary condition (see Figure 4-a). As shown in Figure 4-b, for a slice of the flue-wall of thickness “dx”, the heat balance equation can be written as the total heat coming into the gas control volume is equal to the heat leaving the control volume, which can be described using the following equation [1-8]:

$$\begin{aligned}
 & \overbrace{(\dot{Q}_{gi} - \dot{Q}_{go})}^{\text{flue gas}} - \overbrace{\dot{Q}_{ng}}^{\text{infiltrated air}} - \overbrace{(\dot{Q}_{sg} - \dot{Q}_{gs})}^{\text{Heat transfer from flue gas to wall}} + \overbrace{\dot{Q}_{fg}}^{\text{Heat provided by the fuel}} + \overbrace{\dot{Q}_{vg}}^{\text{Heat provided by the volatiles combusted}} \\
 & + \overbrace{\dot{Q}_{cg}}^{\text{Heat provided by the packing coke combusted}} - \overbrace{(\dot{Q}_{lf} + \dot{Q}_{la})}^{\text{Heat loss to atmosphere and foundation}} = 0
 \end{aligned} \tag{2}$$

Substituting physical expression of the terms mentioned in the Eq. (2), it can be expressed as:

1. For the preheating sections

$$\begin{aligned}
 & \overbrace{\dot{m}_g C_{pg} \frac{dT_g}{dx}}^{\text{flue gas}} + \overbrace{\eta_1 \dot{m}_c H_c}^{\text{Heat provided by the coke}} + \overbrace{\eta_2 (\dot{m}_{tar} H_{tar} + \dot{m}_{CH_4} H_{CH_4} + \dot{m}_{H_2} H_{H_2})}^{\text{Heat provided by the volatiles combusted}} \\
 & - \overbrace{\dot{m}_n C_{pg} (T_g - T_\infty)}^{\text{infiltrated air}} - \overbrace{2h_T D_{flue} (T_g - T_w)}^{\text{Heat transfer from flue gas to wall}} - \overbrace{Wh_{equiv} (T_g - T_\infty)}^{\text{Heat loss to atmosphere and foundation}} = 0
 \end{aligned} \tag{3}$$

2. For the firing sections

$$\begin{aligned}
 & \overbrace{\dot{m}_g C_{pg} \frac{dT_g}{dx}}^{\text{flue gas}} + \overbrace{\eta_1 \dot{m}_c H_c}^{\text{Heat provided by the coke}} + \overbrace{\eta_3 \dot{m}_f H_f}^{\text{Heat provided by the fuel}} \\
 & - \overbrace{\dot{m}_n C_{pg} (T_g - T_\infty)}^{\text{infiltrated air}} - \overbrace{2h_T D_{flue} (T_g - T_w)}^{\text{Heat transfer from flue gas to wall}} - \overbrace{Wh_{equiv} (T_g - T_\infty)}^{\text{Heat loss to atmosphere and foundation}} = 0
 \end{aligned} \tag{4}$$

3. For the cooling sections

$$\begin{aligned}
 & \overbrace{\dot{m}_g C_{pg} \frac{dT_g}{dx}}^{\text{flue gas}} + \overbrace{\eta_1 \dot{m}_c H_c}^{\text{Heat provided by the coke}} - \overbrace{2h_T D_{flue} (T_g - T_w)}^{\text{Heat transfer from flue gas to wall}} \\
 & - \overbrace{Wh_{equiv} (T_g - T_\infty)}^{\text{Heat loss to atmosphere and foundation}} = 0
 \end{aligned} \tag{5}$$

Where,

- $\eta_1$  Percentage of packing coke that combusts, %
- $\eta_2$  Percentage of volatile release that combusts in the flue, %
- $\eta_3$  Combustion efficiency, %
- $W$  Flue width, m
- $P_{flue}$  Equivalent perimeter of the flue, m

$T_g$	Gas temperature, °C
$h_T$	Total heat transfer coefficient (Convective and Radiative), W/m <sup>2</sup> . °C
$\dot{m}_g$	Gas mass flow in the flue, kg/m. s
$\dot{m}_f$	Fuel injection per unit furnace length, kg/m. s
$\dot{m}_v$	Volatiles release rate per unit furnace length, kg/m. s
$c_{pg}$	Specific heat of the gas, J/kg. °C
$T_w$	Wall temperature, °C
$H_f$	Fuel heats of reaction, J/kg
$H_v$	Fuel and volatiles gases heats of reaction, J/kg
$h_{equiv}$	Equivalent heat transfer coefficient; considering the conductive resistance of the top and bottom solid materials, and convective- radiative heat transfer from top and bottom, W/m <sup>2</sup> . °C

The total heat transfer coefficient  $h_T$  is given as the sum of convective and radiative heat transfer coefficients. During the baking process, the mass flow rate of the flue-gas inside the flue wall is a function of the draft level, the design of the flue channel and sealing of the furnace at the sources of the air infiltration such as head wall openings (placing coolers or exhaust manifolds), peep-hole openings (placing burners), porous media (packing coke) and cracks through the brick and concrete flue tops. The green anodes are heat treated in anode baking furnace during the pre-heating and firing zones with the heat provided by the pitch volatiles and fuel combustion respectively. The volatile matters in green anodes are composed of methane, hydrogen and tar. The purpose of the baking process is to convert the coal tar pitch binder into high quality binder coke which holds the filler coke particles together. The amount of volatile gasses released is a function of the anode temperature and mass of the stored volatiles in the green anode. The volatile release rate can be expressed as follows:

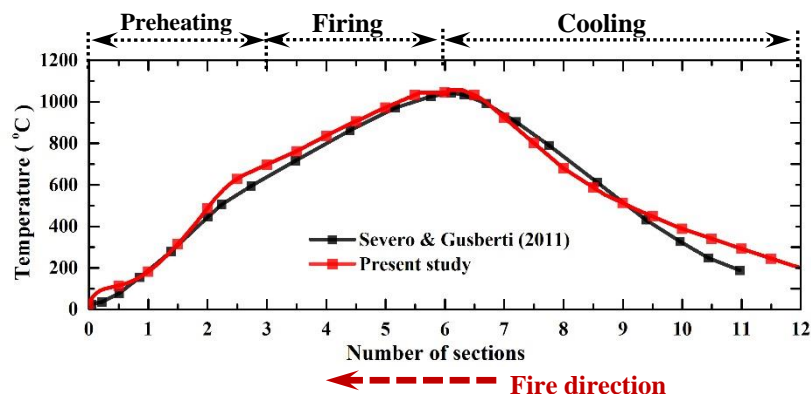
$$\dot{m}_v = \frac{\partial m_v}{\partial T_a} \frac{\partial T_a}{\partial t} = \frac{\partial m_v}{\partial t} \quad (6)$$

### 2.3. Numerical Implementation

The model is developed based on a source code written in our laboratory to simulate the entire carbon anode baking process considering most of the simultaneous transient phenomena, in a simplified manner though realistic. Central-difference approximation is used for discretizing the spatial derivatives of the heat equation, and forward-difference approximation for the temporal derivative. To make the model computationally less intensive, the explicit method is adopted. The grid independence test is carried out. Since the explicit method is conditionally stable, the following stability criteria based on types of nodes. The gas equation is solved using Euler explicit method. The grid independence test (GIT) is carried by varying the temporal and spatial grids and monitoring anode final temperature. The temperature dependent material properties are considered and the values are the same as that of reported by Gusberri & Savero (2011).

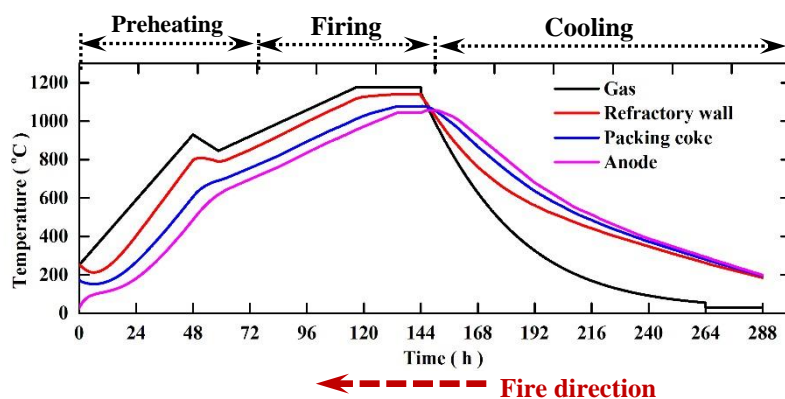
## 3. Results and Discussion

Figure 4 shows the comparison between the calculated anode average temperature with that of reported by Severo and Gusberti (2011). It can be observed that there is a good agreement between the two results.



**Figure 4. Comparison of calculated and reported anode average temperature.**

During the anode baking process, the main concern is to maintain the prescribed temperature curves. The heat-up rate of the anode should not exceed the critical range. It takes typically 24–48 hours for anodes to reach the flue-gas temperature. Hence, considering the anode temperature as the input signal for the control system of the baking process is not feasible. Therefore, the pre-defined anode temperature curve has to be translated into the flue gas temperature curve. Figure 5 shows the calculated flue-gas, refractory wall, packing coke, and anode average temperature distribution obtained.



**Figure 5. Gas, flue-wall and anode average temperature.**

Figure 6 shows effects of varying  $FC$ ,  $T_{g-soaking}$ , and  $t_{g-soaking}$  on anode average temperature for the whole baking process.

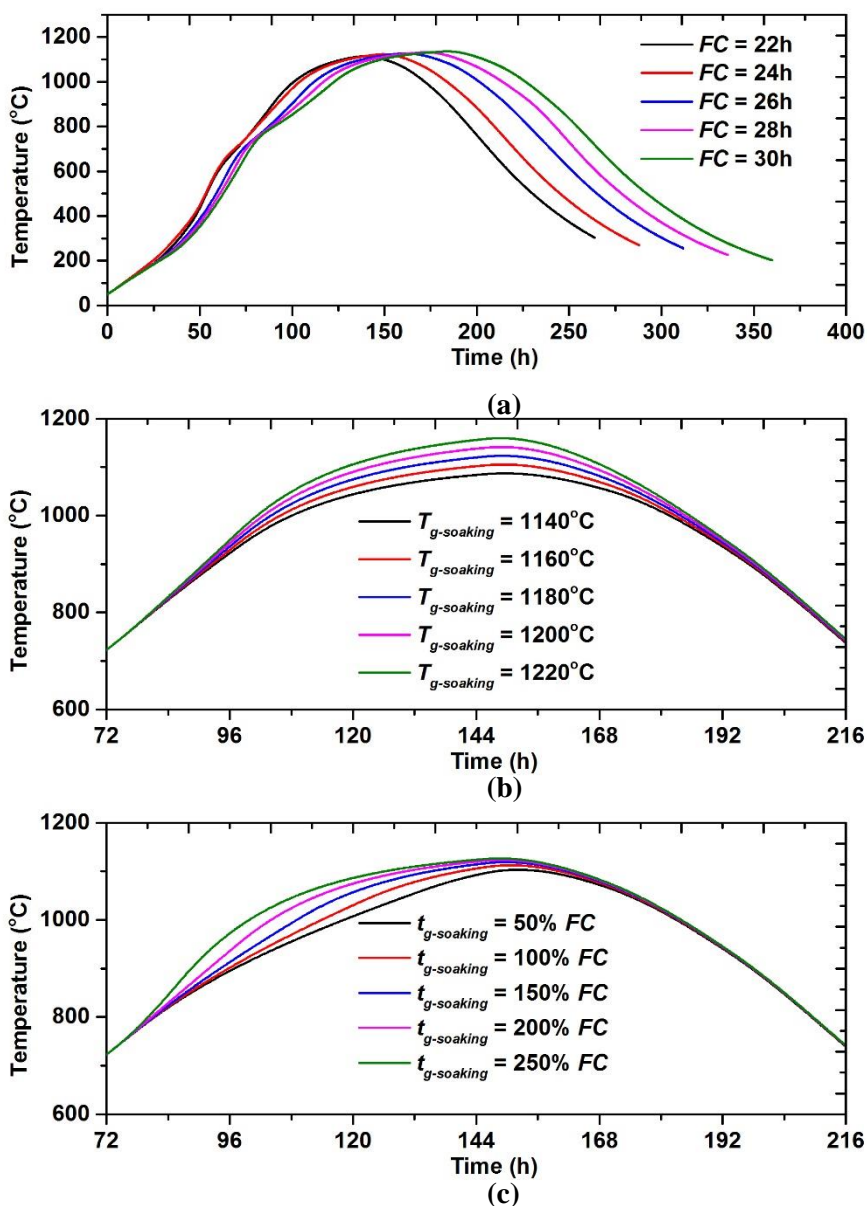


**Figure 6.** Anode average temperature for a) for  $T_{g-soaking} = 1180\text{ }^{\circ}\text{C}$  and  $t_{g-soaking} = 200\%FC$ , b) for  $FC = 24\text{ h}$  and  $t_{g-soaking} = 200\%FC$ , b) for  $FC = 24\text{ h}$  and  $T_{g-soaking} = 1180\text{ }^{\circ}\text{C}$ .

Table 1 shows anode maximum, minimum and average temperature for  $FC\ 24\text{h}$ ,  $T_{g-soaking} = 1140\text{ }^{\circ}\text{C}$  and  $t_{g-soaking} = 50\%$  of  $FC$ . Generally, anodes are in the pit on the top of each other in three or more layers (in  $z$ -direction). So, in addition to calculating the whole anode-pack average temperature, the average temperature of each anode layer is calculated separately. To estimate baking uniformity, two threshold temperature are introduced as  $T_{underbaked} = 1050\text{ }^{\circ}\text{C}$  and  $T_{overbaked} = 1150\text{ }^{\circ}\text{C}$ , and percentage of anode final temperature contour below  $T_{underbaked}$  is considered to be a under-baked area (UBA) and above  $T_{overbaked}$  is assumed to be an over-baked area (OBA). The degree of overbaking and under-baking can be better understood considering UBA, OBA in addition to anode maximum, minimum and average temperature. Table 2 provides UBA, OBA, fuel and volatiles combustion per ton of anodes to be produced. The

results provided in these two tables will be the base case for the comparisons made in the figure 7.

**Table 1. Anode Final Temperature for  $FC = 24h$ ,  $T_{g-soaking} = 1140$  °C and  $t_{g-soaking} = 50$  % of  $FC$  (base case results for Figure 7).**

Parameter	T- Maximum for the whole pack (°C)	T- Minimum for the whole pack (°C)	T- Average for whole the pack (°C)	T- Average for the bottom layer (°C)	T- Average for the middle layer (°C)	T- Average for the top layer (°C)
Value	1106.5	860.4	1071	1058.3	1105.2	1050.2

**Table 2. Energy consumption and baking uniformity parameters for  $FC = 24h$ ,  $T_{g-soaking} = 1140$  °C and  $t_{g-soaking} = 50$  % of  $FC$  (base case results for Figure 7).**

Parameter	<i>OBA</i> (%)	<i>UBA</i> (%)	<i>STD</i> (°C)	Fuel Consumption (GJ/ton of Anode)	Volatiles Consumption (GJ/ton of Anode)
Values	0	23	49	1.634	2.229

**Error! Reference source not found.** Figure 7 shows effects of varying  $T_{g-soaking}$  (1140 to 1220 °C) and  $t_{g-soaking}$  (50% of  $FC$  to 250% of  $FC$ ) for the  $FC$  of 24h. As shown in **Error! Reference source not found.**, the results are compared with the base case (see Table 1 & Table 2), and the increase in all the output parameters are illustrated in 2D contour plots. It can be observed that at lower  $T_{g-soaking}$  and  $t_{g-soaking}$ , fuel consumption is low which is desirable but, the anode final temperature is not high enough, and under-baked volume is as high as 27% of the total volume. Similarly, for very high  $T_{g-soaking}$  and  $t_{g-soaking}$ , the fuel consumption is high and at the middle anodes experience very high temperature. Moreover, it can be observed that by an increase in  $T_{g-soaking}$  and  $t_{g-soaking}$ ,  $STD$  increases as well which seem to be desirable. However, as mentioned earlier at lower  $T_{g-soaking}$  and  $t_{g-soaking}$ , despite lower  $STD$ , the  $UBA$  is very high and reduces by an increase in soaking time and temperature.

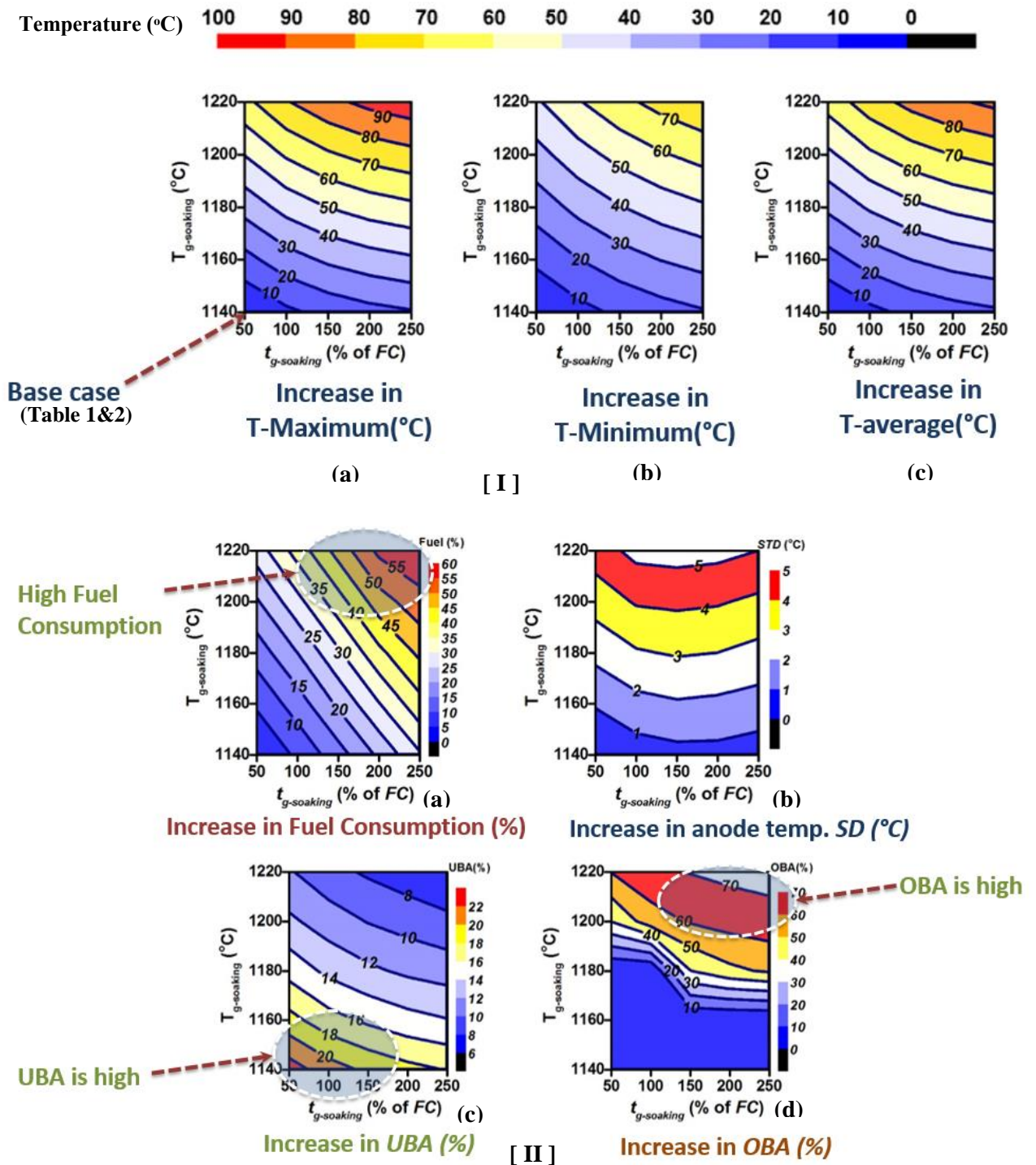


Figure 7. Effect of varying  $T_{g-soaking}$  and  $t_{g-soaking}$ , for  $FC = 24h$ , on [I] a)  $\Delta T_{a-max}$  (°C), b)  $\Delta T_{a-min}$  (°C), c)  $\Delta T_{a-avg}$  (°C), [II] a) Increase in fuel consumption (%), b) STD (°C), c) UBA (%), d) OBA (%).

Table 3 shows anode maximum, minimum and average temperature for FC 22h,  $T_{g-soaking} = 1140$  °C and  $t_{g-soaking} = 50$  % of FC. Table 4 provides UBA, OBA, fuel and volatiles combustion per ton of anodes to be produced. Results illustrated in Table 3 and 4 is considered the base case for the comparison made in the Figure 8.

**Table 3. Anode Final Temperature for  $FC = 22h$ ,  $T_{g-soaking} = 1140$  °C and  $t_{g-soaking} = 50$  % of  $FCI$  (base case results for Figure 8).**

Parameter	T- Maximum for the whole pack (°C)	T- Minimum for the whole pack (°C)	T- Average for whole the pack (°C)	T- Average for the bottom layer (°C)	T- Average for the middle layer (°C)	T- Average for the top layer (°C)
Value	1094.8	846.4	1058.3	1044.1	<b>1093.5</b>	1038

**Table 4. Energy consumption and baking uniformity parameters for  $FC = 22h$ ,  $T_{g-soaking} = 1140$  °C and  $t_{g-soaking} = 50$  % of  $FCI$  (base case results for Figure 8).**

Parameter	<i>OBA</i> (%)	<i>UBA</i> (%)	<i>STD</i> (°C)	Fuel Consumption (GJ/ton of Anode)	Volatiles Consumption (GJ/ton of Anode)
Values	0	27.7	50.4	1.593	2.177

Figure 8 show effects of varying  $FC$  and  $t_{g-soaking}$  for the  $T_{g-soaking}$  of 1180°C. The increase in anode final temperature can be observed by an increase in  $FC$  and  $T_{g-soaking}$ . At  $t_{g-soaking} = 1140$ °C and 1160°C the *OBA* is relatively high.

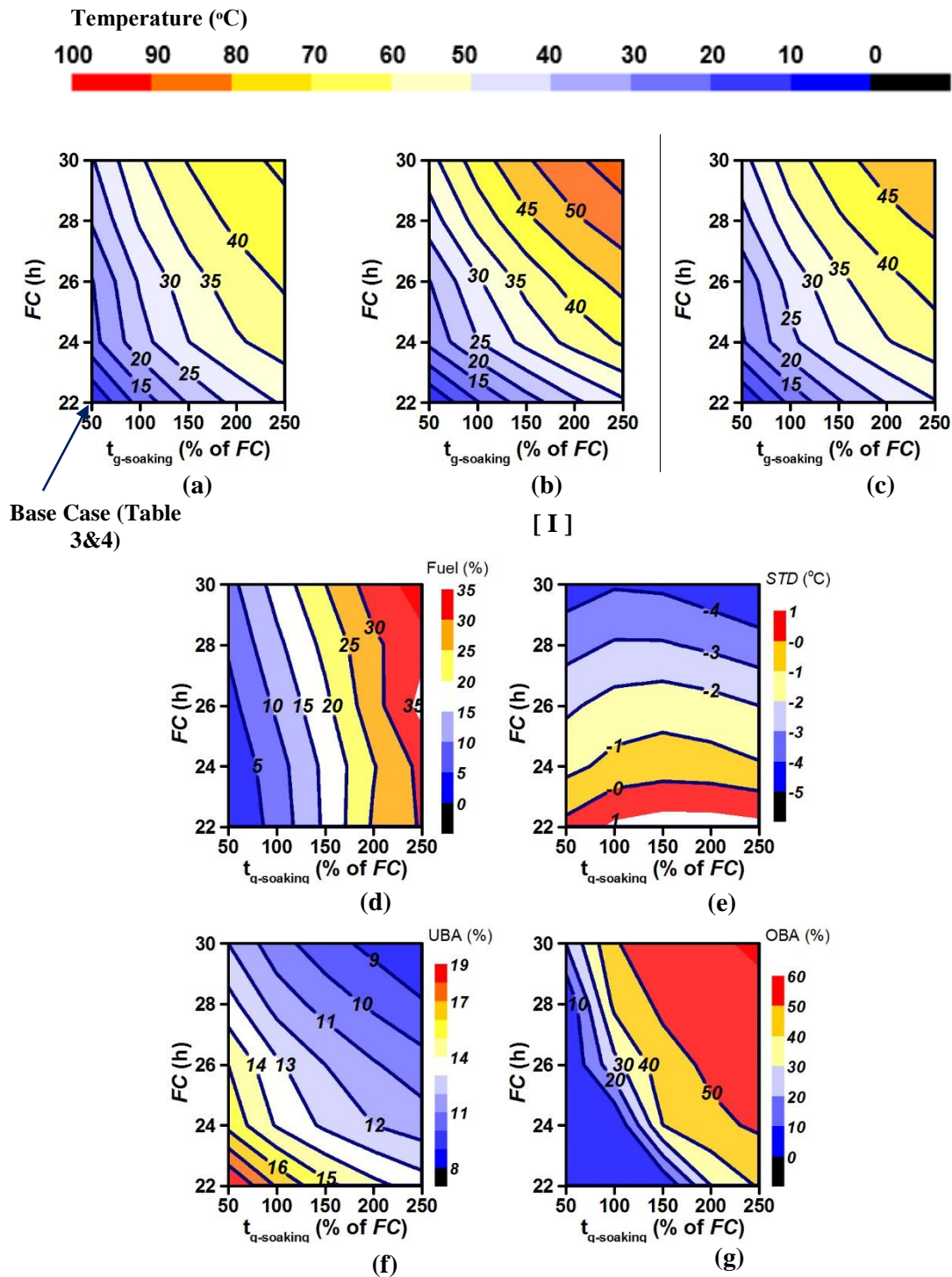


Figure 8. Effect of varying  $FC$  and  $t_{g-soaking}$  for  $T_{g-soaking} = 1180$  °C on [I] a)  $\Delta T_{a-max}$  (°C), b)  $\Delta T_{a-min}$  (°C), c)  $\Delta T_{a-avg}$ , [II] d) Fuel consumption (%), e)  $STD$  (°C), f)  $UBA$  (%) and g)  $OBA$  (%).

#### 4. Conclusions

In the present study, a numerical model is developed for the anode baking process. Using this numerical model, effects of varying  $FC$ , with different flue-gas soaking temperature and soaking time are studied. The results are expressed in terms of fuel consumption, and anode maximum, minimum and average temperature for each layer of anode-pack separately. Furthermore, the baking uniformity for each case is investigated by calculating anode temperature standard deviation, and percentage of under-baked and over-baked areas. Considering multiple factors such as anode temperature, fuel consumption and baking homogeneity, desirable combinations of  $FC$ ,  $T_{g-soaking}$  and  $t_{g-soaking}$  can be located on illustrated two-dimensional contour maps. Finally, for varying  $FC$  and  $t_{g-soaking}$ , and fixed  $T_{g-soaking}$ , it is observed that by an increase in  $FC$ , baking homogeneity can be improved with a slight increase in fuel consumption; however, it reduces the furnace production which should be taken into consideration at the same time.

#### 5. Acknowledgements

The authors acknowledge the support from the Emirates Global Aluminium (EGA).

#### 6. References

1. R. Bui, A. Charette, T. Bourgeois, Simulating the process of carbon anode baking used in the aluminum industry, *Metallurgical Transactions B*, 15 (1984) 487-492.
2. L. Zhang, C. Zheng, M. Xu, Simulating the heat transfer process of horizontal anode baking furnace, *Developments in Chemical Engineering and Mineral Processing*, 13 (2005) 447-458.
3. D.S. Severo, & Gusberti, V., User-friendly software for simulation of anode baking furnaces, in: Proceeding of 10th Australian conference, 2011.
4. Akhtar, R. J., Meier, M. W., Sulger, P. O., Fischer, W. K., Friedrich, R., & Janousch, T. (2012). Anode Quality and Bake Furnace Performance of EMAL. *Light Metals*, 1175-1179.
5. Tajik AR, Shamim T, Al-Rub RK, Zaidani M. Performance Analysis of a Horizontal Anode Baking Furnace for Aluminum Production. In ICTEA: International Conference on Thermal Engineering 2017 Mar 15 (Vol. 2017).
6. Tajik AR, Shamim T, Al-Rub RK, Zaidani M. Two-Dimensional CFD Simulations of a Flue-wall in the Anode Baking Furnace for Aluminum Production. *Energy Procedia*. 2017 May 31;105:5134-9.
7. Tajik AR, Shamim T, Al-Rub RK, Zaidani M. Process Modelling of a Horizontal Anode Baking Furnace for Aluminum Production, The International Committee for Study of Bauxite, Alumina & Aluminum – ICSOBA2016.
8. Zaidani M, Al-Rub RA, Tajik AR, Shamim T. Effects of Flue Wall Deformation on Aluminum Anode Baking Homogeneity and Temperature Distribution, The International Committee for Study of Bauxite, Alumina & Aluminum – ICSOBA2016.
9. Zaidani M, Al-Rub RA, Tajik AR, Shamim T. Investigation of the Flue-wall Aging Effects on the Anode Baking Furnace Performance. In ICTEA: International Conference on Thermal Engineering 2017 Mar 15 (Vol. 2017).
10. Tajik AR, Hindasageri V. A numerical investigation on heat transfer and emissions characteristics of impinging radial jet reattachment combustion (RJRC) flame. *Applied Thermal Engineering*. 2015 Oct 5;89:534-44.
11. Tajik AR, Shamim T, Abu Al-Rub R, Zaidani M, Numerical Investigation of Turbulent Diffusion Flame in the Aluminum Anode Baking Furnace Employing Presumed PDF, The 9th International Conference on Applied Energy (ICAE2017).

12. Zaidani M, Al-Rub RA, Tajik AR, Shamim T, 3D Multiphysics Model of the Effect of Flue-wall Deformation on the Anode Baking Homogeneity, The 9th International Conference on Applied Energy (ICAE2017).
13. Tajik AR, Shamim T, Abu Al-Rub R, Zaidani M, Transient Process Modelling of Carbon Anode Baking Furnace for Aluminum Production, *ASME 2017 Summer Heat Transfer Conference*.
14. Zaidani M, Al-Rub RA, Tajik AR, Shamim T, Computational Modeling of the Effect of Flue-wall Deformation on the Carbon Anode Quality for Aluminum Production, *ASME 2017 Summer Heat Transfer Conference*.

